

# Using the Best Linear Approximation With Varying Excitation Signals for Nonlinear System Characterization

Alireza Fakhrizadeh Esfahani, *Student Member IEEE*, Johan Schoukens, *Fellow, IEEE*,  
and Laurent Vanbeylen, *Member, IEEE*

**Abstract**—Block oriented model structure detection is quite desirable since it helps to imagine the system with real physical elements. In this work we explore experimental methods to detect the internal structure of the system, using a black box approach. Two different strategies are compared and the best combination of these is introduced. The methods are applied on two real systems with a static nonlinear block in the feedback path. The main goal is to excite the system in a way that reduces the total distortion in the measured frequency response functions to have more precise measurements and more reliable decision about the structure of the system.

**Index Terms**—Nonlinear systems, Best linear approximation, nonlinear distortion, Bussgang’s theorem, Optimal input design, central composite design (CCD), structure detection, nonlinear feedback,

## I. INTRODUCTION

**F**REQUENCY response function (FRF) measurement, is very interesting for modelling and identification. FRF analysis is used not only for modelling but also it can be used to get insight in the internal structure of the system under test. Since nonlinear (NL) identification usually is a very time consuming procedure, it is highly desirable to carefully select an appropriate model structure prior to the actual identification. In this article, we study block-oriented systems [1], and [2], consisting of interconnected dynamic linear blocks and static nonlinear blocks. In [1] different block-oriented structure systems, such as, Wiener-Hammerstein, parallel Wiener-Hammerstein and nonlinear unity feedback systems are studied in the time domain. These structures are analyzed by using spectral analysis of Volterra series expansion of the block structured non-linear system in [3]. A complete review of these methods can be found in [4], and [2].

Here the internal structure of block oriented systems is explored, for which already a large number of possible internal

structures can be present. In this work the focus is on the detection of the nonlinear structure by using the Best Linear Approximation (BLA), such as, the presence of NL feedback. The FRF of the BLA [5] is measured for different excitation signal’s properties. In Billings and Fakhouri [6], it is proposed to use nonzero mean Gaussian distributed signals in combination with a correlation analysis, for recognizing a nonlinear system with a unity feedback structure. In [7], the standard deviation (STD) and bandwidth of the excitation signals are changed to study the internal structure of the system by using the BLA analysis. In [8] (This paper is the extension of the article, which authors presented in the PMTC conference in 2015), in contrast to [7], amplitude (STD value) level, and/or DC level (mean value, offset or operating point) of a full-band random phase multisine within frequency band of interest are varied to analyze the block oriented nonlinear structure. In this study, the idea of varying DC and STDs, as proposed in [8] is extended to find an optimal selection of DC and STD levels, to have a minimum amount of distortions and therefore a set of high-quality BLA measurements (which, on turn, can serve to get insight in the nonlinear system). The proposed method is based on the Central Composite Design (CCD) method [9]. The novelty of the article is the extraction of an eigen-path using CCD, which gives the best<sup>1</sup> strategy for varying the DC, and STD levels of the input signal.

Multisines are used for exciting systems under test. Multisines are in the class of Gaussian signals by increasing the number of frequencies lines asymptotically [5]. This periodic signal gives the same BLA as a filtered Gaussian (a colored Gaussian process) excitation with the same bandwidth.

Simultaneously with the measurement of the BLA, a non-parametric analysis of the nonlinear distortions is done. On the basis of these results the potential of both properties is discussed. A method is proposed for which both properties (DC and STD levels) are varied. By using this method, FRFs have less distortion, and the structure detection and furthermore any post-processing calculation will be more reliable.

The internal nonlinear structure of the system can be identified, by changing the excitation’s characteristic values, the DC and STD levels. Information about the nonlinear structure of the system can be retrieved by finding the BLA, with different

<sup>1</sup>The strategy is optimal in the sense that - in a local approximation in the DC/STD space - the magnitudes of the total distortions on the BLA are jointly minimized.

The authors thank Johan Pattyn for the design and realization of the setup in 5(b).

This work was supported in part by the Fund for Scientific Research (FWO-Vlaanderen), by the Flemish Government (Methusalem), the Belgian Government through the Inter university Poles of Attraction (IAP VII) Program, and by the ERC advanced grant SNLSID, under contract 320378.

Using the Best Linear Approximation With Varying Excitation Signals for Nonlinear System Characterization

Alireza Fakhrizadeh Esfahani; Johan Schoukens; Laurent Vanbeylen

IEEE Transactions on Instrumentation and Measurement

Year: 2016, Volume: 65, Issue: 5 Pages: 1271 - 1280

DOI: 10.1109/TIM.2015.2504079

<https://ieeexplore.ieee.org/document/7373634/>

©IEEE 2016

experiments through varying the excitation signal's DC and STD values.

In Section II, Bussgang's theorem [10], (providing information about the BLA of static systems), is proved to be valid for an excitation contains DC value. It is shown, that varying the DC level of the excitation signal has less nonlinear distortion contributions at the BLA. So it is a good idea to vary the DC level, to retrieve information about the nonlinear structure of the system through variations of the BLA.

By calculating and fitting a parametric model on the FRF, we can follow the behavior of the poles and zeros and choose the best internal structure [11].

The main contributions of this work are:

- Extension of Bussgang's theorem to include nonzero mean Gaussian inputs.
- Structure detection for block oriented models, through varying the input properties.
- Analysis of the pole-zero behavior of different internal structures.
- Finding the best strategy for varying the DC and STD level of the signal to measure different high quality BLAs that can be used to detect the block oriented structure of the system.

A proposition to Bussgang's theorem for non-zero mean excitations is presented in Section II. In Section III, block oriented models are introduced. In Section IV, the concept of the best linear approximation is reviewed. The structure detection method is explained in Section V. In Section VI an experimental method for selecting the best DC and STD levels of the signal is introduced. Systems under study and measurement results are given in Section VII and VIII. Section IX, concludes the paper.

## II. BUSSGANG'S THEOREM FOR NON-ZERO MEAN EXCITATIONS

Structure detection, based on the BLA of block oriented models, needs to study the BLA of the static nonlinearity (SNL), a memoryless function block. It can be done through the Bussgang's theorem, which simply stated, means that a SNL system excited with Gaussian signals has a constant BLA (static, frequency-independent). However, Bussgang did not provide the proof in case the input has non-zero mean. Here, it is needed to analyze the BLAs at different DC levels (non-zero mean input).

According to Bussgang's theorem, [10] if the input signal of a SNL system, is a stationary (colored) zero mean Gaussian process, the BLA of a SNL block is a constant. The static nonlinearity should fulfill the following property:

$$\int_{-\infty}^{\infty} x g_x(x) e^{-\frac{x^2}{2}} dx < \infty \quad (1)$$

This condition covers a large class of functions such as, functions with a finite number of discontinuities, and functions with a finite number of discontinuous derivatives.

Here we will show, that Bussgang's theorem is also valid for non-zero mean input.

**Proposition 1.** Assume  $p(t)$  to be a stationary (colored) nonzero mean Gaussian process, and  $q(t) = g_p(p(t))$ , then

$$R_{pq}(\tau) = k R_{pp}(\tau) \quad (2)$$

here,  $R_{uv}$  and  $R_{uu}$  are the cross- and auto-covariance respectively.

*Proof:* It is assumed, that the input process  $p(t)$  is a Gaussian process, with a non-zero mean  $\mathbb{E}\{p_t\} = \mu_p = p_{DC}$

$$p(t) = \mu_p + x(t) \quad (3)$$

where  $\mu_p$  is the mean value of  $p(t)$  and  $x(t)$  is a stationary zero-mean, Gaussian process (See Fig. 1). It can be remarked that the SNL  $g_p(\bullet)$  can be redefined in terms of an offset and a function  $g_x(\bullet)$ :

$$g_p(p) = g_x(p - \mu_p) \quad (4)$$

or equivalently:

$$g_x(x) = g_p(x + \mu_p) \quad (5)$$

Since  $\mathbb{E}\{x(t)\} = 0$ , Bussgang's theorem applies to  $g_x(\bullet)$  [10]:

$$R_{xq}(\tau) = k R_{xx}(\tau) \quad (6)$$

Using the equations corresponding to the block diagram in Fig. 1, a result similar to (6) can be obtained in terms of the signal  $p$ :

$$R_{pq}(\tau) = k R_{pp}(\tau) \quad (7)$$

This fact is the simple consequence of

$$\begin{aligned} R_{pq}(\tau) &= \mathbb{E}\{(p(t+\tau) - \mathbb{E}\{p(t+\tau)\})(q(t) - \mathbb{E}\{q(t)\})\} \\ &= \mathbb{E}\{(x(t+\tau) + \mu_p - \mathbb{E}\{x(t+\tau) + \mu_p\}) \\ &\quad (q(t) - \mathbb{E}\{q(t)\})\} \\ &= \mathbb{E}\{(x(t+\tau) - \mathbb{E}\{x(t+\tau)\})(q(t) - \mathbb{E}\{q(t)\})\} \\ &= R_{xq}(\tau) \end{aligned} \quad (8)$$

and

$$\begin{aligned} R_{pp}(\tau) &= \mathbb{E}\{(p(t+\tau) - \mathbb{E}\{p(t+\tau)\})(p(t) - \mathbb{E}\{p(t)\})\} \\ &= \mathbb{E}\{(p(t+\tau) - \mu_p)(p(t) - \mu_p)\} \\ &= \mathbb{E}\{x(t+\tau)x(t)\} \\ &= \mathbb{E}\{(x(t+\tau) - \mathbb{E}\{x(t+\tau)\})(x(t) - \mathbb{E}\{x(t)\})\} \\ &= R_{xx}(\tau) \end{aligned} \quad (9)$$

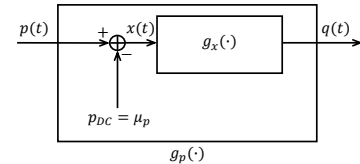


Figure 1. Block diagram of a SNL system with nonzero mean input.

In this work multisine excitations are used. Multisines, are among the class of Gaussian signals, (as number of the excited frequencies approaches to infinity). Gaussian signals are separable, for separable processes, and Bussgang's theorem, also known as the invariance property holds [1], [12].

From proposition 1, it follows that Bussgang's theorem is valid also for nonzero mean excitations. So the best linear

approximation of an SNL system, even with nonzero mean inputs is a constant  $k$  (see also (11) and (12)) depending on the mean (DC) and the variance (STD<sup>2</sup>) of  $p(t)$ . This fact will be used in the sequel to detect the internal structure of block oriented models (see Section V).

### III. BLOCK ORIENTED NONLINEAR MODELS

Block oriented nonlinear models can be defined as an interconnection of static nonlinear (SNL) and linear time invariant blocks [1], [2]. Three types of block oriented systems that are considered in this paper are:

- A Wiener-Hammerstein (WH) system:

Is defined as the cascade connection of two linear dynamic systems and a static nonlinearity in between.

- A parallel WH system:

Parallel branches of different WH systems

- A nonlinear feedback system:

A branch of a WH system at the feedback and a linear time invariant block at the feedforward path. The WH system can be located either in the feedforward or in the feedback path [13]. In Fig. 2, the three different block oriented systems, which are considered in this paper, are shown.

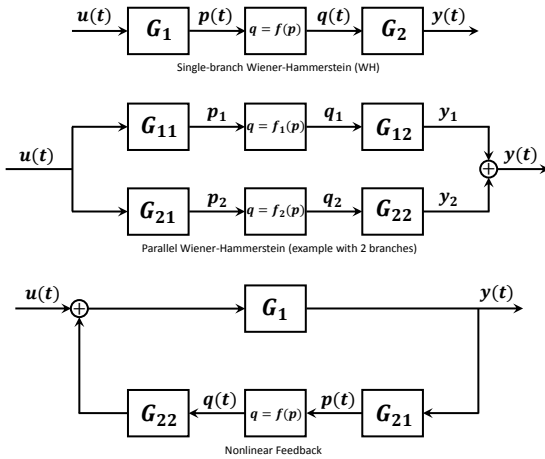


Figure 2. A few examples of block oriented nonlinear structures.

### IV. THE BEST LINEAR APPROXIMATION

The best linear approximation (BLA) is a tool to measure the frequency response function [5], [14], [15] of a nonlinear dynamic system (assuming that the response to a periodic input is periodic with the same period as the input). Here the BLA is used to analyze the block oriented internal structure of the system. In this section the BLA is defined in the first part, and next the estimation method is explained.

#### A. Definition

The best linear approximation is defined as [5], [15], [16]

$$G_{BLA}(j\omega) = \arg \min_{G(j\omega)} \mathbb{E}_u \left\{ |Y(j\omega) - G(j\omega)U(j\omega)|^2 \right\} \quad (10)$$

where  $Y(j\omega)$ ,  $G(j\omega)$ , and  $U(j\omega)$  are the real output of the system, the model, and the input of the system respectively.

$G_{BLA}(j\omega)$  is the BLA of the system.  $\mathbb{E}_u$  denotes the mathematical expectation with respect to the random input.

It can be assumed that a nonlinear dynamic system, is replaced by the BLA plus a nonlinear distortion term  $y_s(t)$  (see Fig. 3).  $y_s(t)$  is uncorrelated with  $u(t)$ , but not independent (for a detailed discussion see Sec. 3.4 of [5] or [17], [18]). The following equations hold (see Section II) in the time and frequency domain, respectively:

$$R_{yu} = g_{BLA} \star R_{uu}, \quad (11)$$

$$S_{yu} = G_{BLA} S_{uu}. \quad (12)$$

where  $R_{yu}$ , and  $R_{uu}$  are input-output cross correlation, and input auto-correlation, respectively.  $\star$  stands for the convolution operation, and  $g_{BLA}$  is the BLA in the time domain (the inverse Fourier transform of  $G_{BLA}$ ).  $S_{yu}$ , and  $S_{uu}$  are input-output cross power, and input auto-power spectra, respectively.

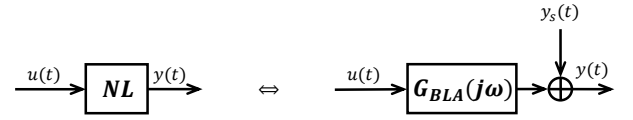


Figure 3. Analogy between the NL system and the BLA.

The BLA depends on the class of inputs to which  $u$  belongs. Here, the class of band-limited Gaussian noise signals, with a certain mean value (DC) and standard deviation (STD), are used.

#### B. Estimation

To estimate the BLA easily, it is proposed to excite the system with Gaussian distributed excitations (see Section II) for example, random phase multisine signals. More precisely, with random phase multisines [5], the calculated BLA has less uncertainty, compared with random excitations [5], [19]. Two methods to analyze the NL distortion with the BLA spectrum, are called the robust method and the fast method [5], [19].

These methods allow one to separate the noise and the nonlinear distortion  $y_s(t)$ . Hence from the multisine measurement, the FRF of the BLA, the noise, and the nonlinear contributions can be quantified non-parametrically in the frequency domain [5], [19]. In this work the robust method is adopted [19], [5].

The total distortion  $\hat{\sigma}_{G_{BLA}}^2$ , includes the stochastic nonlinear distortion  $\hat{\sigma}_{G_s}^2$  on the BLA, and the noise contribution  $\hat{\sigma}_{G_{BLA,n}}^2$ . By exciting the system with a periodic excitation, the user is able to estimate the noise contribution  $\hat{\sigma}_{G_{BLA,n}}^2$ . By subtracting the noise contribution from the total distortion, the nonlinear distortion is calculated. The mentioned quantities are calculated as follows:

$$\hat{U}^{[m]}(j\omega_k) = \frac{1}{P} \sum_{p=1}^P U^{[m,p]}(j\omega_k) \quad (13)$$

$$\hat{Y}^{[m]}(j\omega_k) = \frac{1}{P} \sum_{p=1}^P Y^{[m,p]}(j\omega_k) \quad (14)$$

$$\hat{\sigma}_{\hat{U}^{[m]}}^2(j\omega_k) = \sum_{p=1}^P \frac{|U^{[m,p]}(j\omega_k) - \hat{U}^{[m]}(j\omega_k)|^2}{P(P-1)} \quad (15)$$

## V. STRUCTURE DETECTION

By analyzing the BLA variations that take place, for varying DC and STD (standard deviation of the  $u(t)$ ) levels of the excitation signal, the internal structure of the system is detected. Applying Bussgang's theorem to the structures in Fig. 2, the BLA is given below.

It is possible to select one out of 3 candidate model structures by varying the excitation signal's characteristic values. For Gaussian distributed excitation signal for all structures in Fig. 2, and changing the DC and STD of the signal [7] for each mentioned structure, we have the following results

- Wiener-Hammerstein (WH) systems:

$$G_{BLA}(j\omega) = kG_1(j\omega)G_2(j\omega) \quad (29)$$

In this structure

$$G_1 = \frac{N_1}{D_1}, G_2 = \frac{N_2}{D_2} \rightarrow G_{BLA} = k \frac{N_1 N_2}{D_1 D_2} \quad (30)$$

where, according to Bussgang's theorem,  $k$  is the best linear approximation of the static nonlinearity  $q = f(p)$ . By changing the DC and STD of the excitation signal,  $k$  changes, but poles and zeros of the  $G_{BLA}$  don't change.

- Parallel Wiener-Hammerstein systems (example with 2 branches):

$$G_{BLA} = G_{1BLA} + G_{2BLA} \quad (31)$$

Here the following equations hold

$$\begin{cases} G_{11} = \frac{N_{11}}{D_{11}}, G_{12} = \frac{N_{12}}{D_{12}} \rightarrow G_{1BLA} = k_1 G_{11}(j\omega) G_{12}(j\omega) \\ G_{21} = \frac{N_{21}}{D_{21}}, G_{22} = \frac{N_{22}}{D_{22}} \rightarrow G_{2BLA} = k_2 G_{21}(j\omega) G_{22}(j\omega) \end{cases} \quad (32)$$

$$G_{BLA} = k_1 G_{11}(j\omega) G_{12}(j\omega) + k_2 G_{21}(j\omega) G_{22}(j\omega) \quad (33)$$

$$= k_1 \frac{N_{11}}{D_{11}} \frac{N_{12}}{D_{12}} + k_2 \frac{N_{21}}{D_{21}} \frac{N_{22}}{D_{22}} \quad (34)$$

$$= \frac{k_1 N_{11} N_{12} D_{21} D_{22} + k_2 N_{21} N_{22} D_{11} D_{12}}{D_{11} D_{12} D_{21} D_{22}} \quad (35)$$

where  $k_1$  and  $k_2$  are the BLAs of the static nonlinearity in the first and second branches respectively. Here it can be seen that the overall BLA has a pole set of the union of pole sets of each branch. But the zeros are different from the zeros of branches. So by changing the DC and RMS levels, zeros move but poles don't. The detailed identification procedure can be found in [20].

- Nonlinear feedback:

As a first approximation<sup>2</sup> we have that:

$$G_{BLA} \cong \frac{G_1(j\omega)}{1 + G_1(j\omega)G_{BLAfb}} \quad (36)$$

In this case the relations are

$$\begin{cases} G_1 = \frac{N_1}{D_1} \\ G_{21} = \frac{N_{21}}{D_{21}}, G_{22} = \frac{N_{22}}{D_{22}} \rightarrow G_{BLAfb} = k G_{21}(j\omega) G_{22}(j\omega) \end{cases} \quad (37)$$

<sup>2</sup>It should be noted, that the input of the SNL in the NL feedback case is not Gaussian anymore. As long as the input's amplitude is small, the input of the SNL block tends to be Gaussian. In this case the BLA is the same as the  $\epsilon$ -approximation [11].

$$\hat{\sigma}_{\hat{Y}^{[m]}}^2(j\omega_k) = \sum_{p=1}^P \frac{|Y^{[m,p]}(j\omega_k) - \hat{Y}^{[m]}(j\omega_k)|^2}{P(P-1)} \quad (16)$$

$$\hat{\sigma}_{\hat{Y}^{[m]}\hat{U}^{[m]}}^2(j\omega_k) = \sum_{p=1}^P \frac{(Y^{[m,p]}(j\omega_k) - \hat{Y}^{[m]}(j\omega_k))(\overline{U^{[m,p]}(j\omega_k) - \hat{U}^{[m]}(j\omega_k)})}{P(P-1)} \quad (17)$$

$$\hat{G}^{[m]}(j\omega_k) = \frac{\hat{Y}^{[m]}(j\omega_k)}{\hat{U}^{[m]}(j\omega_k)} \quad (18)$$

$$\hat{G}_{BLA}(j\omega_k) = \sum_{m=1}^M \frac{\hat{G}^{[m]}(j\omega_k)}{M} \quad (19)$$

$$\hat{\sigma}_{\hat{G}_{BLA}}^2(j\omega_k) = \sum_{m=1}^M \frac{|G^{[m]}(j\omega_k) - \hat{G}_{BLA}(j\omega_k)|^2}{M(M-1)} \quad (20)$$

$$\hat{\sigma}_{\hat{U},n}^2(j\omega_k) = \frac{1}{M} \sum_{m=1}^M \hat{\sigma}_{\hat{U}^{[m]}}^2(j\omega_k) \quad (21)$$

$$\hat{\sigma}_{\hat{Y},n}^2(j\omega_k) = \frac{1}{M} \sum_{m=1}^M \hat{\sigma}_{\hat{Y}^{[m]}}^2(j\omega_k) \quad (22)$$

$$\hat{\sigma}_{\hat{Y}\hat{U},n}^2(j\omega_k) = \frac{1}{M} \sum_{m=1}^M \hat{\sigma}_{\hat{Y}^{[m]}\hat{U}^{[m]}}^2(j\omega_k) \quad (23)$$

$$\hat{S}_{U_0 U_0}(j\omega_k) = \frac{1}{M} \sum_{m=1}^M \left( |\hat{U}^{[m]}(j\omega_k)|^2 - \hat{\sigma}_{\hat{U},n}^2(j\omega_k) \right) \quad (24)$$

$$\hat{S}_{Y_0 Y_0}(j\omega_k) = \frac{1}{M} \sum_{m=1}^M \left( |\hat{Y}^{[m]}(j\omega_k)|^2 - \hat{\sigma}_{\hat{Y},n}^2(j\omega_k) \right) \quad (25)$$

$$\hat{S}_{Y_0 U_0}(j\omega_k) = \frac{1}{M} \sum_{m=1}^M \left( \hat{Y}^{[m]} \overline{\hat{U}^{[m]}}(j\omega_k) - \hat{\sigma}_{\hat{Y}\hat{U},n}^2(j\omega_k) \right) \quad (26)$$

$$\hat{\sigma}_{\hat{G}_{BLA,n}}^2(j\omega_k) = \frac{|\hat{G}_{BLA}(j\omega_k)|^2}{M} \cdot \left( \frac{\hat{\sigma}_{\hat{Y},n}^2(j\omega_k)}{\hat{S}_{Y_0 Y_0}(j\omega_k)} + \frac{\hat{\sigma}_{\hat{U},n}^2(j\omega_k)}{\hat{S}_{U_0 U_0}(j\omega_k)} - 2\text{Re}\left(\frac{\hat{\sigma}_{\hat{Y}\hat{U},n}^2(j\omega_k)}{\hat{S}_{Y_0 U_0}(j\omega_k)}\right) \right) \quad (27)$$

$$\hat{\sigma}_{\hat{G}_s}^2(j\omega_k) = M(\hat{\sigma}_{\hat{G}_{BLA}}^2(j\omega_k) - \hat{\sigma}_{\hat{G}_{BLA,n}}^2(j\omega_k)) \quad (28)$$

with  $M$  is the number of experiments,  $P$  is the number of periods,  $U^{[m,p]}(j\omega_k)$  and  $Y^{[m,p]}(j\omega_k)$  are the Fourier transform of one period of the input and output signals in one experiment respectively (for a detailed discussion see Sec. 6.1 of [19]).

TABLE I  
POLE ZERO BEHAVIOR OF CONSIDERED STRUCTURES.

	Zeros	Poles
WH	Don't change	Don't change
WH. Parallel	Change	Don't Change
NL Feedback	Don't change	Change

$$G_{BLA} \cong \frac{G_1(j\omega)}{1 + G_1(j\omega)kG_{21}(j\omega)G_{22}(j\omega)} \quad (38)$$

$$= \frac{\frac{N_1}{D_1}}{1 + k \frac{N_1}{D_1} \frac{N_{21}}{D_{21}} \frac{N_{22}}{D_{22}}} \quad (39)$$

$$= \frac{N_1 D_{21} D_{22}}{D_1 D_{21} D_{22} + k N_1 N_{21} N_{22}}. \quad (40)$$

Here  $k$  is the BLA of the static nonlinearity in the feedback path. It is seen that the overall BLA has zeros of the union of the zero set of feedforward path and the pole set of the feedback path. By varying the excitation signal's characteristics (e.g. DC and STD) the overall zeros don't change, but the poles change. In the special case where  $G_{21} = G_{22} = 1$  the zeros of the closed loop system are the same as the zeros of feedforward path.

The results of this section are collected in Table I. This table allows to obtain an idea of a possible internal NL structure in an early phase (prior to the actual modeling) starting from BLAs. E.g., if the estimated poles of the BLA are depending on DC or STD, it can readily be determined that nonlinear feedback is present.

The reader should be aware that the mentioned pole-zero behaviors are necessary conditions for the presence of the related structure, in other words there are different structures other than above with the same behavior of pole-zero. This is discussed in [11].

## VI. OPTIMIZING, SIGNAL'S CHARACTERISTICS

In this section an experimental algorithm is introduced to find a set of DC and STD levels of the input signal to have less distorted BLAs. The first part of the proposed method uses the Central Composite Design (CCD) [9] approach<sup>3</sup>. Then on the saddle point of the quadratic model the eigen-path gives the set of experiments, in which both the DC and STD levels are simultaneously varied.

It is expected, that the behavior of a nonlinear system is changed with varying DC and STD (amplitude) of the signal. Also, by exciting the system with low-amplitude signals (STD), the noise distortion is typically more significant in the BLA. This gives either a hyper-bola, convex, or concave surface to the MSEs of BLAs, which can be approximated by a quadratic model. This quadratic model for MSEs is controlled by the DC and STD level. The eigen-path on the extremum point of the surface gives the set of experimental points. This gives a set of BLAs with less distortion levels. The algorithm is as follows:

- 1) Normalize the DC and STD according to their range  $\Delta DC$  (or  $DC_{max} - DC_{min}$ ) and  $\Delta STD$  (or  $STD_{max} - STD_{min}$ ):

$$x_1 = \frac{DC - DC_C}{\Delta DC / 2} \quad (41)$$

$$x_2 = \frac{STD - STD_C}{\Delta STD / 2} \quad (42)$$

where  $DC_C$  and  $STD_C$  are the center point of the CCD experiment. Make the following experiment plan, where each row corresponds the settings of an experiment:

$$X_{plan} = \begin{matrix} & x_1 & x_2 \\ \left. \begin{matrix} +1 & -1 \\ +1 & +1 \\ -1 & -1 \\ -1 & +1 \\ \sqrt{2} & 0 \\ -\sqrt{2} & 0 \\ 0 & \sqrt{2} \\ 0 & -\sqrt{2} \\ 0 & 0 \\ \vdots & \vdots \\ 0 & 0 \end{matrix} \right\} & & \end{matrix} \quad l \text{ times} \quad (43)$$

- 2) At each experimental point for the DC and STD level of the excitation, estimate the BLA and its MSE (Mean Square Error which is defined on the total distortion  $\hat{\sigma}_{\hat{G}_{BLA}}^2$ ):

$$MSE = \frac{1}{f_{k_N} - f_{k_1}} \int_{f_{k_1}}^{f_{k_{N_{ex}}}} \hat{\sigma}_{\hat{G}_{BLA}}^2 df \quad (44)$$

where,  $f_{k_1}$ , and  $f_{k_{N_{ex}}}$  are the first and the last excited frequencies respectively in the multisine signal.

- 3) Build a full quadratic model for MSEs, by using a linear least square fit (regression with  $X_{plan}$  as regressor and the MSEs as dependent vector):

$$\hat{MSE} = A_{20}x_1^2 + A_{11}x_1x_2 + A_{02}x_2^2 + A_{10}x_1 + A_{01}x_2 + A_{00} \quad (45)$$

- 4) By doing multiple ( $l$ ) experiments at the center point, it gives the ability to measure the noise level in MSEs. Based on that, the uncertainty of the estimated parameters also can be estimated:

$$RSS = \sum_{i=1}^n (MSE_{m_i} - \hat{MSE}_i) \quad (46)$$

$$\text{Var}(MSE) = RSS / (n - p) \quad (47)$$

$$\text{Cov}(\hat{A}_i) = (X_m^T X_m)^{-1} \text{Var}(MSE) \quad (48)$$

where RSS is the residual sum of squares,  $\hat{MSE}$  is the vector of predicted MSEs, the subscript  $m$  represents the measured values of each variable,  $n$  is the number of all experiments, and  $p$  is the degree of freedom (number of unknown parameters  $A_i$ ), that here is equal to the number of parameters in the model.

- 5) Calculate the signal to noise ratio ( $t_i$ ) for each coefficient according to:

$$t_i = \frac{\hat{A}_i}{\text{STD} \hat{A}_i} \quad (49)$$

<sup>3</sup>Standard CCD method is explained through steps 1-6.

where  $\hat{A}_i$  is the estimated coefficients and  $\text{STD}\hat{A}_i$  is:

$$\text{STD}(\hat{A}_i) = \sqrt{\text{diag}(\text{Cov}(\hat{A}_i))} \quad (50)$$

- 6) Drop the coefficients with low absolute signal to noise ratio ( $|t_i|$ ). As a rule of thumb, it is recommended to drop the coefficients with  $t$ -values less than 3,
- 7) Find the extremum point of the surface by solving:

$$\begin{bmatrix} 2A_{20} & A_{11} \\ A_{11} & 2A_{02} \end{bmatrix} \begin{bmatrix} x_1^* \\ x_2^* \end{bmatrix} + \begin{bmatrix} A_{10} \\ A_{01} \end{bmatrix} = \begin{bmatrix} 0 \\ 0 \end{bmatrix} \quad (51)$$

- 8) Transfer (45) to the new point  $(x_1^*, x_2^*)$
- 9) This new equation can be written as:

$$\text{MSE}_{ex} = \begin{bmatrix} \tilde{x}_1 & \tilde{x}_2 \end{bmatrix} \overbrace{\begin{bmatrix} \tilde{A}_{20} & \tilde{A}_{11}/2 \\ \tilde{A}_{11}/2 & \tilde{A}_{02} \end{bmatrix}}^Q \begin{bmatrix} \tilde{x}_1 \\ \tilde{x}_2 \end{bmatrix} \quad (52)$$

$$= \tilde{A}_{20}\tilde{x}_1^2 + \tilde{A}_{11}\tilde{x}_1\tilde{x}_2 + \tilde{A}_{02}\tilde{x}_2^2 \quad (53)$$

where  $\tilde{x}_i = x_i - x_i^*$  ( $i = 1, 2$ ) is a new transferred variable.

- 10) The eigenvector of the matrix  $Q$  corresponding to the lowest eigenvalue determines the line (through  $x^*$ ) along which the MSE varies the least, and therefore delivers different BLAs of the highest quality. This gives the best strategy for doing the experiments.

## VII. SYSTEMS UNDER STUDY

Two nonlinear feedback systems are considered in this study, a nonlinear mass spring damper (NL-MSD) system (see Fig. 4 and Fig. 5(a)), and a linear system with a multiplication operation in the feedback path (NL-XFB) (Fig. 5(b)). Both systems are implemented as electronic circuits. The proposed methodology will be applied to measurements of these devices (see Section VIII).

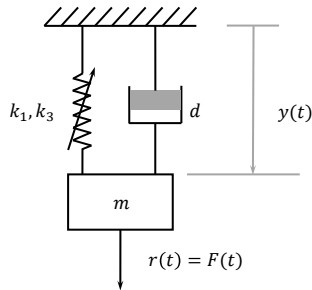


Figure 4. Nonlinear mass spring damper with a cubic term as hardening effect.

### A. The nonlinear mass spring damper system (NL-MSD)

This system has a spring with a nonlinear cubic term  $k_3y^3$  to model a mechanical hardening spring effect. For this system we have

$$m\ddot{y} + d\dot{y} + k_1y + k_3y^3 = r(t) \quad (54)$$

$$m\ddot{y} + d\dot{y} + k_1y = r(t) - k_3y^3 \quad (55)$$

The equivalent block diagram of this system is shown in Fig. 5(a) (also known as the Silverbox) [21].

### B. The nonlinear system with a multiplication in the feedback path (NL-XFB)

The second system, shown in Fig. 5(b) is composed of a dual amplifier bandpass filter [22] in the forward path with a multiplication at the feedback which is fed by an independent branch from the input with a squaring device (AD835) followed by a generalized impedance converter (GIC)-derived dual-amplifier biquad as a low-pass filter [23].

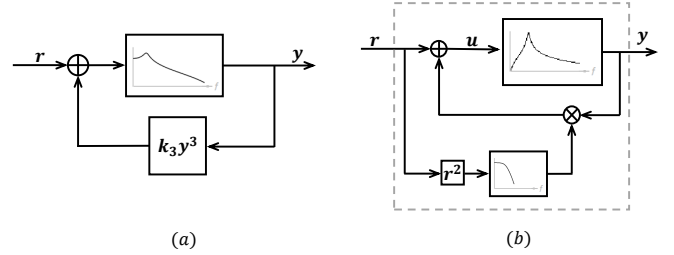


Figure 5. Block diagram of systems under study.

## VIII. MEASUREMENT RESULTS

Two systems under study are excited with random phase multisine signal. The settings for the excitation signal are written in Table II, and measured with Agilent/HP E1430A data acquisition cards. Both systems are excited by an Agilent/HP E1445A arbitrary wave generator (AWG).

### A. Structure Detection

The FRFs (BLAs) of the NL-MSD are plotted in Fig. 6. In the left of this figure, FRFs with different DC level of the excitation signals are shown, while in the right, FRFs are plotted for different STD levels. It is seen that by increasing the input amplitude (STD), the resonance frequency shifts and also the damping changes. This behavior points to pole movements, hence to the presence of a nonlinear feedback [24].

It is seen (in the left) that the total standard deviation ( $\hat{\sigma}_{\hat{G}_{BLA}}$ ) and the noise level ( $\hat{\sigma}_{\hat{G}_{BLA,n}}$ ) are decreased, by increasing the DC level of the input signal. As the DC level is increased, the total standard deviation and noise level are decreased, but as the STD level is increased (see right side of the Fig. 6), the stochastic nonlinear distortion ( $\hat{\sigma}_{\hat{G}_{BLA,n}}$ ) is increased, (as expected, high amplitude hits the nonlinearities more).

Fig. 7 shows a similar picture for the NL-XFB system. In the left side of this figure there are plots of the FRFs with varying the DC level. At the right side, the FRFs are calculated with the different STD levels of the excitation signal. In the varying DC level experiment, the total distortion is decreased, while in the STD sweeping experiment the total distortion has an increasing trend. Therefore it is recommended to use rather the DC sweeping than the varying STD, to detect the internal structure.

Through parametric fitting on frequency response functions, by using Matlab<sup>®</sup> FDIDENT toolbox [25], the movement of

TABLE II  
EXPERIMENT PARAMETERS.

	NL-MSD	NL-XFB
Number of points (per period) ( $N$ )	4883	19531
Number of realizations ( $M$ )	64	16
Number of periods ( $P$ )	4	4
Sampling frequency ( $f_s$ )	2.44 KHz	9.77 KHz
Excited harmonics $k_{ex}$	[3:2:399]	[1:2:4999]
Number of excited frequencies ( $N_{ex}$ )	199	2500
frequency resolution ( $f_0$ )	0.5Hz	0.5Hz

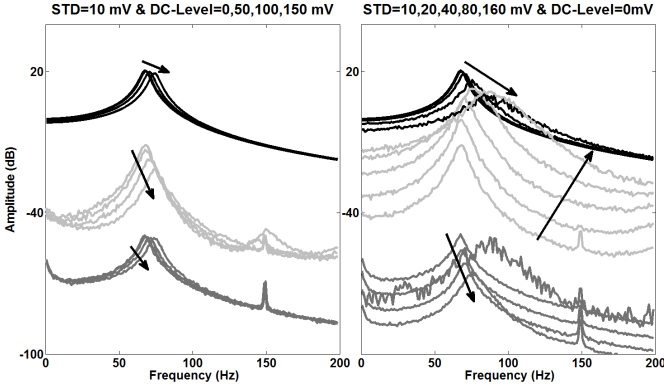


Figure 6. FRFs of the NL-MSD (Silverbox). Bold line:  $\hat{G}_{BLA}$ , light grey:  $\hat{\sigma}_{\hat{G}_{BLA}}$ , and dark grey:  $\hat{\sigma}_{\hat{G}_{BLA},n}$ . Arrows point from low to high DC or STD levels.

poles and zeros can be followed. It is assumed that the NL-MSD system has second order dynamics (without zeros), and the NL-XFB is a second order system with a zero (see the deep antiresonance in Fig. 7 at the frequency 0Hz). In Figs. 8 and 9 the pole-zero locus of systems under study are illustrated. In Fig. 9 the movement of poles have all the same natural frequency. As it is seen in Figs. 8 and 9 the poles move in both systems. So, the presence of the nonlinear feedback can

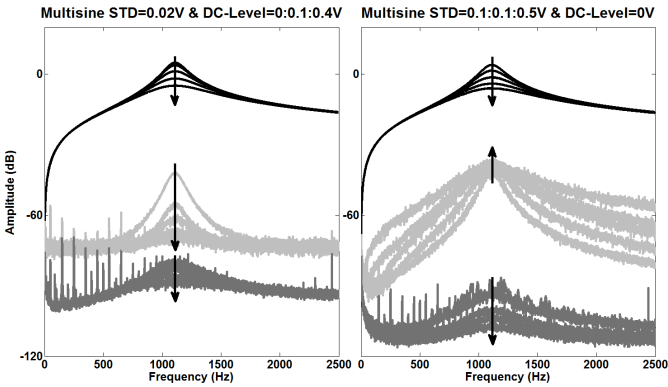


Figure 7. FRFs of the NL-XFB. Arrows point from low to high DC or STD levels. Bold line:  $\hat{G}_{BLA}$ , light grey:  $\hat{\sigma}_{\hat{G}_{BLA}}$ , and dark grey:  $\hat{\sigma}_{\hat{G}_{BLA},n}$ .

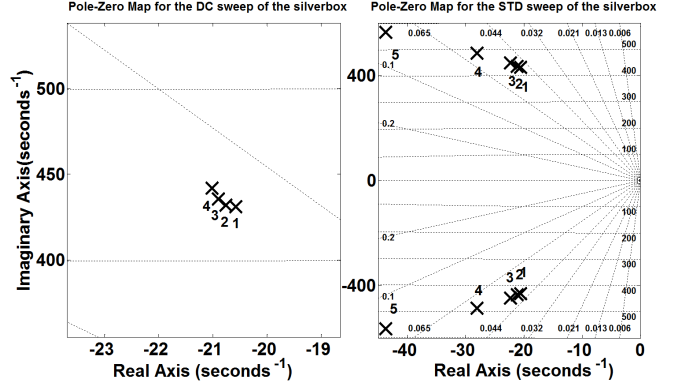


Figure 8. Pole-Zero map of varying DC (left) and varying STD experiments on the NL-MSD system. Labels 1 to 4 correspond to DC and STD levels shown in Fig. 6 (low to high).

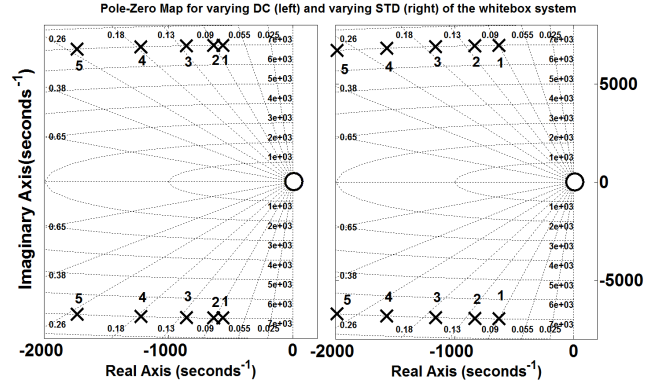


Figure 9. Pole-Zero map of varying DC (left) and varying STD experiments on the NL-XFB system. Labels 1 to 5 correspond to DC and STD levels shown in Fig. 7 (low to high).

be detected in both systems.

In Fig. 8 the pole-zero map of the NL-MSD system by a DC sweep (left), and a STD sweep (right) show pole movements of the system. This behavior suggests again the existence of the feedback branch. Also in Fig. 9, in both cases (STD and DC sweep), the poles are shifting, while the zeros don't change. This behavior allows again one to easily detect the existence of the feedback branch.

### B. Input Optimization

In this part the results of the proposed method for selecting the DC and STD level of the signal are shown. These results are based on the experiments carried out on the NL-MSD system.

1) *Experiments on a grid in the DC-STD plane:* The 11 DC and 16 STD levels are selected according to Table III. For this set of experiments the sampling frequency, number of excited frequency, and the frequency resolution are selected according to the NL-MSD column of Table II. Fig. 10 shows the MSEs (in dB) of all signals with permissible DC and STD levels

of the excitation signal. The results agree with the fact that, by decreasing the STD level, the MSE is decreased because, the noise has more contribution in the total distortion. But by increasing the STD level, the MSEs (dB) are increased, because of the nonlinear contribution of the system. It is clear that varying the DC level of the input signal at a fixed STD level, doesn't have a significant impact on MSE levels.

2) *Proposed method:* The CCD method explained in Section VI was applied to find the best strategy to reach to the minimum value of MSEs, based on only 10 different values of (DC, STD). Fig. 11 shows the contour plot of all the experiments grid (Fig. 10). In this figure squares and the star show the designed experiments according to the matrix in (43). The quadratic surface which is built according to these experiments is plotted in Fig. 12. The dash-line in Fig. 11 shows the best strategy we should select to reach to an FRF with a minimum distortion level. Also this line is shown in Fig. 12, as a white line.

The designed DC and STD levels according to this line are in Table IV. Fig. 13 shows the FRFs of the designed experiment. By comparing this figure with the Fig. 6 (the left side, FRFs for varying DC), the noise contribution is slightly increased but the total and stochastic nonlinear distortions decrease significantly. Moreover, the maximum of the total distortion only varies very slightly, corresponding to slight changes of the MSE on the optimal line. By fitting a parametric model on each FRFs in the optimal experiment we have the poles-zeros of transfer functions. Fig. 14 shows the pole-zero trend of the new experiment.

TABLE III  
SETTINGS FOR FULL GRID MEASUREMENT

DC Levels	0, 10, 20, 30, 40, 50, 60, 70, 80, 90, 100 mV
STD Levels	1, 2, 4, 6, 8, 10, 20, 30, 40, 50, 60, 70, 80, 90, 100, 110 mV

Table IV  
THE DESIGNED EXPERIMENT VALUES (RESULTS OF CCD METHOD)

DC Levels	17, 57, 97, 137, 177 mV
STD Levels	4, 5, 6, 7, 8 mV

## IX. CONCLUSIONS

Busgang's theorem is still valid for nonzero mean excitation signals. By using the Input/Output BLA of a system, with varying input signal properties (DC and STD level), and studying the pole zero behavior of the BLA, we are able to select a block oriented structure out of the 3 different types of internal structures i.e. series, parallel Wiener-Hammerstein systems, and nonlinear feedback structure (see Table I). By changing the DC and STD levels, it is possible to influence the level of the nonlinear and noise distortions. Varying the DC level is preferable to varying the STD, since delivers much higher quality (lower distortion) BLA measurements. An optimal experimental design procedure is proposed, where DC and STD values are varied jointly.

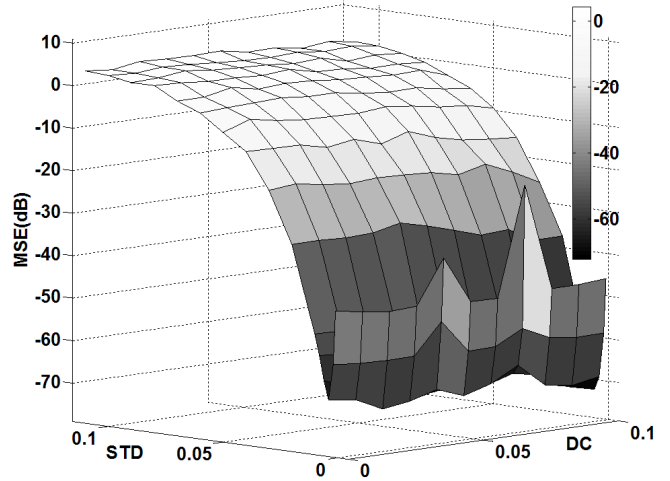


Figure 10. Surface MSE(DC, STD) for the NL-MSD system (DC and STD levels according to Table III): MSE in dB as function of the DC value and the STD.

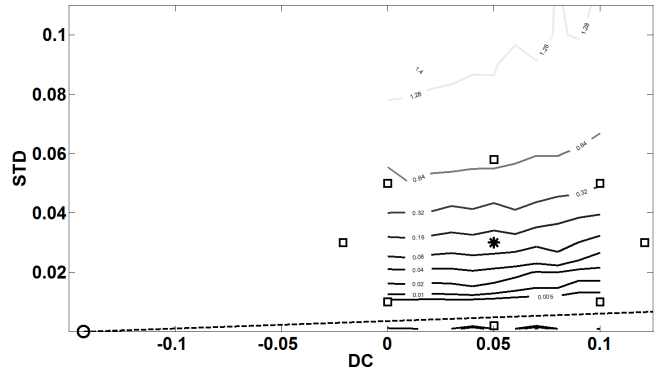


Figure 11. Contour plot of MSEs for grid experiments (Fig. 10). Here MSE scale is linear. Squares (□) and the asterisk (\*) are the CCD designed experiment points. The circle (o) at the far left bottom of the figure is the calculated extremum point of the quadratic model. The dash-line is the eigenpath which is selected as the best strategy.

## REFERENCES

- [1] S. A. Billings and S. Y. Fakhouri, "Identification of systems containing linear dynamic and static nonlinear elements," *Automatica*, vol. 18, pp. 15–26, 1982.
- [2] F. Giri and E.-W. Bai, *Block-oriented Nonlinear System Identification*. Springer-Verlag, 2010.
- [3] S. A. Billings and K. M. Tsang, "Spectral analysis of block structured non-linear systems," *Mechanical Systems and Signal Processing*, vol. 4, pp. 117–130, 1990.
- [4] R. Haber and H. Unbehauen, "Structure identification of nonlinear dynamic systems—a survey on input/output approaches," *Automatica*, vol. 26, pp. 651–677, 1990.
- [5] R. Pintelon and J. Schoukens, *System Identification a Frequency Domain Approach*. John Wiley & Sons, Inc., 2012.
- [6] S. A. Billings and S. Y. Fakhouri, "Identification of non-linear unity feedback systems," University of Sheffield, Tech. Rep., 1978.



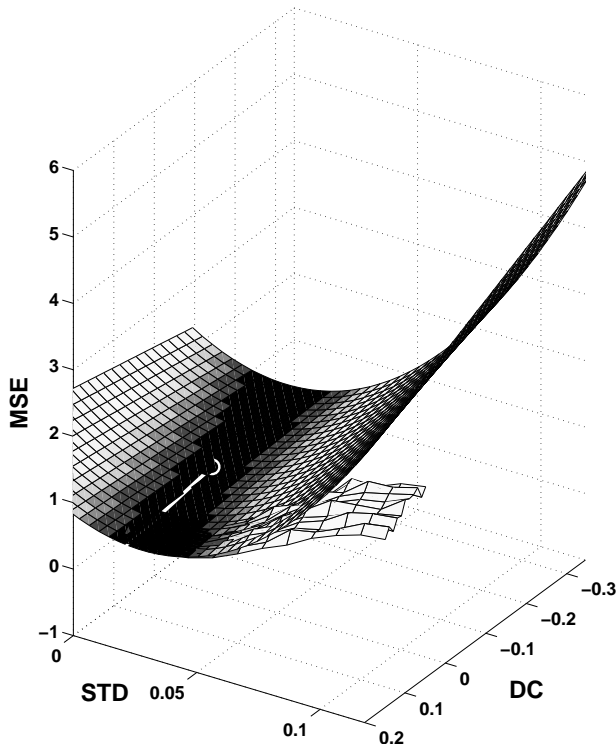


Figure 12. The extracted 2<sup>nd</sup> order surface for the MSEs (with fine meshes), the grid experiment surface (with coarse meshes), the eigen-path (the white line) and the saddle point of the modeled surface (the white circle).

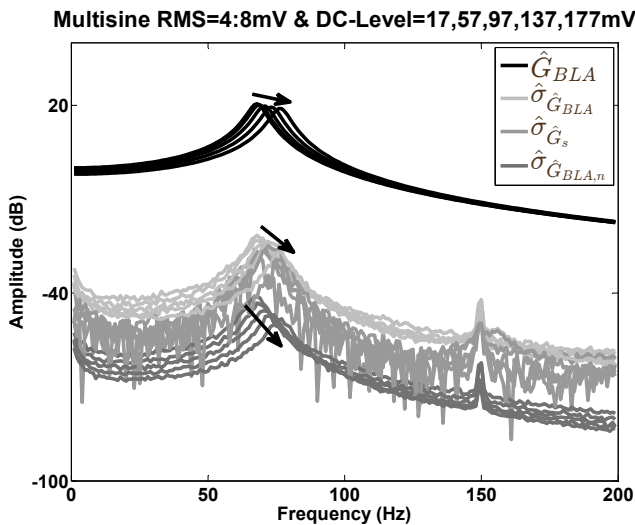


Figure 13. FRFs of the designed excitation signal. Arrows point from the lowest value of DC and STD levels to the highest. Bold line:  $\hat{G}_{BLA}$ , light grey:  $\hat{\sigma}_{\hat{G}_{BLA}}$ , dark grey:  $\hat{\sigma}_{\hat{G}_{BLA,n}}$ , and medium grey is the stochastic nonlinear distortion  $\hat{\sigma}_{\hat{G}_s}$ .

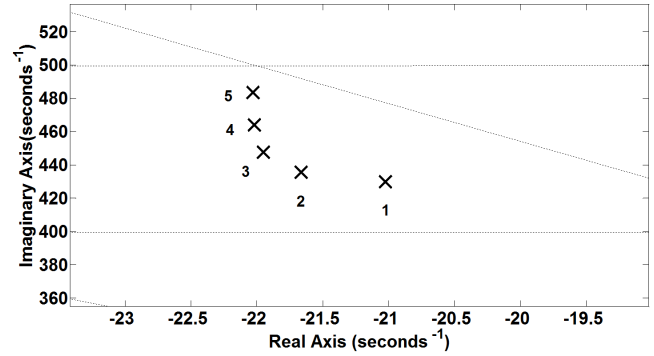


Figure 14. Pole-Zero map of the designed experiment for the NL-MSD system.

2015, pp. 234–239.

- [9] W. G. H. George E. P. Box, J. Stuart Hunter, *Statistics for experimenters: design, discovery, and innovation*. John Wiley & Sons, Inc., 2005.
- [10] J. J. Bussgang, “Crosscorrelation functions of amplitude-distorted gaussian signals,” Res. Lab. Electron., Mass. Inst. Technol., Cambridge, MA, MIT Tech Rep. P. No 216, Tech. Rep., 1952.
- [11] J. Schoukens, R. Pintelon, Y. Rolain, M. Schoukens, K. Tiels, L. Vanbeylen, A. V. Mulders, and G. Vandersteen, “Structure discrimination in block-oriented models using linear approximations: A theoretic framework,” *Automatica*, vol. 53, pp. 225–234, 2015.
- [12] A. H. Nuttall, “Theory and application of the separable class of random processes,” MIT, Tech. Rep., 1958.
- [13] J. Schoukens, L. Gomme, W. V. Moer, and Y. Rolain, “Identification of block-structured nonlinear feedback system, applied to a microwave crystal detector,” *IEEE Trans. Instrum. Meas.*, vol. 57, pp. 1734–1740, 2008.
- [14] J. S. Bendat and A. G. Piersol, *Engineering Application of Correlation and Spectral Analysis*. New York, NY, USA: Wiley, 1980.
- [15] J. Schoukens, R. Pintelon, T. Dobrowiecki, and Y. Rolain, “Identification of linear systems with non-linear distortions,” *Automatica*, vol. 41, pp. 491–504, 2005.
- [16] M. Enqvist and L. Ljung, “Linear approximations of nonlinear fir systems for separable input processes,” *Automatica*, vol. 41, pp. 459–473, 2005.
- [17] R. Pintelon and J. Schoukens, “Measurement and modelling of linear systems in the presence of non-linear distortions,” *Mechanical systems and signal processing*, vol. 16.5, pp. 785–801, 2002.
- [18] J. Schoukens, T. Dobrowiecki, and R. Pintelon, “Parametric and non-parametric identification of linear systems in the presence of nonlinear distortions—a frequency domain approach,” *Automatic Control, IEEE Transactions on*, vol. 43, no. 2, pp. 176–190, Feb 1998.
- [19] J. Schoukens, R. Pintelon, and Y. Rolain, *Mastering System Identification in 100 Exercises*, L. Hanzo, Ed. John Wiley & Sons, Inc., 2012.
- [20] M. Schoukens, K. Tiels, M. Ishteva, and J. Schoukens, “Identification of parallel wiener-hammerstein systems with decoupled static nonlinearity,” *IFAC world congress*, 2014.
- [21] J. Schoukens, J. G. Nemeth, P. Crama, Y. Rolain, and R. Pintelon, “Fast approximate identification of nonlinear systems,” *Automatica*, vol. 39(7), pp. 1267–1274, 2003.
- [22] H. Zumbahlen, Ed., *Linear Circuit Design Handbook*. Newnes, 2008.
- [23] W.-K. Chen, Ed., *The Circuits and Filters Handbook*. CRC Press, 2002.
- [24] J. Schoukens, J. Swevers, J. Paduart, D. Vaes, K. Smolders, and R. Pintelon, “Initial estimate for block structure nonlinear systems with feedback,” *Proc. Int. Symp. Nonlinear Theory Appl.*, pp. 622–625, 2005.
- [25] I. Kollifir, R. Pintelon, J. Schoukens, and G. Simon, “Implementing a graphical user interface and automatic procedures for easier identification and modeling,” *IEEE Instrum. Meas. Magazine*, pp. 19–26, 2003.

[7] L. Lauwers, J. Schoukens, R. Pintelon, and M. Enqvist, “A nonlinear block structure identification procedure using frequency response function measurements,” *IEEE Trans. Instrum. Meas.*, vol. 57, pp. 2257–2264, 2008.

[8] F. E. Alireza, J. Schoukens, and L. Vanbeylen, “Design of excitations for structure discrimination of nonlinear systems, using the best linear approximation,” in *Proc. IEEE Instrum. Meas., Technol. Conf.*, May